

SV2 Renders Primed Synaptic Vesicles Competent for Ca^{2+} -Induced Exocytosis

Wen-Pin Chang¹ and Thomas C. Südhof^{1,2,3,4}

Departments of ¹Neuroscience and ²Molecular Genetics, University of Texas Southwestern Medical Center, Dallas, Texas 75390-9111, ³Neuroscience Institute and Department of Molecular and Cellular Physiology, Stanford University School of Medicine, Palo Alto, California 94304-5543, and ⁴Howard Hughes Medical Institute at University of Texas Southwestern Medical Center and Stanford University School of Medicine

Synaptic vesicle protein 2 (SV2), one of the first synaptic vesicle proteins identified, is characterized by multiple transmembrane regions that exhibit homology to sugar transporters, and by a highly glycosylated intravesicular sequence. Deletion of SV2 causes postnatal lethality in mice, primarily because of fulminant epilepsy. At the cellular level, deletion of SV2 impairs neurotransmitter release, but its function is unknown, and even the exact point at which release is affected in SV2-deleted synapses remains unclear. Using electrophysiological approaches, we now examine at what step in exocytosis the deletion of SV2 impairs release. Our data demonstrate that deletion of SV2 produces a decrease in evoked synaptic responses without causing changes in mini frequency, mini amplitude, the readily releasable pool of vesicles, or the apparent Ca^{2+} sensitivity of vesicle fusion. These findings indicate that a previously unidentified step may couple priming of synaptic vesicles to Ca^{2+} triggering of fusion, and that SV2 acts in this step to render primed synaptic vesicles fully Ca^{2+} responsive. To investigate the structural requirements for this function of SV2, we used rescue experiments. We demonstrate that conserved charged residues within the transmembrane regions and the intravesicular glycosylation of SV2 are required for its normal folding and trafficking. In contrast, the conserved putative synaptotagmin-binding sequence of SV2 is fully dispensable. Viewed together, these observations suggest that SV2 functions in a maturation step of primed vesicles that converts the vesicles into a Ca^{2+} - and synaptotagmin-responsive state.

Key words: synaptic vesicle; membrane fusion; synaptotagmin; readily releasable pool; neurotransmitter release; short-term synaptic plasticity

Introduction

Synaptic transmission is initiated when an action potential triggers neurotransmitter release from presynaptic nerve terminals by synaptic vesicle exocytosis (Katz, 1969). Traditionally, synaptic vesicle exocytosis is divided into four sequential stages: First, neurotransmitters are transported into synaptic vesicles, then vesicles dock at the active zone (docking), and prime at the plasma membrane (priming). Finally, primed vesicles are triggered for exocytosis by Ca^{2+} (Südhof, 2004).

SV2 is a component of all vertebrate synaptic vesicles (Buckle and Kelly, 1985). Three SV2 isoforms, SV2A, SV2B, and SV2C, were identified (Bajjalieh et al., 1992; Feany et al., 1992; Gingrich et al., 1992; Bajjalieh et al., 1993; Janz and Südhof, 1999). All SV2 proteins contain 12 transmembrane regions (TMRs) with N- and C-terminal cytoplasmic sequences and a large intravesicular loop that is *N*-glycosylated. Comparisons of different SV2 isoforms show that the TMRs and cytoplasmic loops are highly conserved,

while the intravesicular loop, although *N*-glycosylated in all SV2 isoforms, exhibits little homology (Janz and Südhof, 1999). SV2A is expressed ubiquitously, while SV2B is present in a more restricted forebrain pattern (Bajjalieh et al., 1994), and SV2C is concentrated in caudal brain regions (Janz and Südhof, 1999). A distantly related synaptic vesicle protein called SVOP contains a similar transmembrane structure as SV2, but lacks its long cytoplasmic and highly glycosylated intravesicular loops (Janz et al., 1998).

SV2 and SVOP exhibit significant homology to bacterial and eukaryotic sugar transporter proteins (Bajjalieh et al., 1992; Feany et al., 1992; Gingrich et al., 1992), indicating that SV2 and SVOP may serve as transporter proteins. In support of this hypothesis, all SV2 isoforms contain two charged residues in TMR1 that are 3 aa apart, placing them to the same face of an α -helix. Moreover, the enormous glycosylation of SV2 proteins suggested that they could function as chemiosmotic stabilizers of synaptic vesicles (Scranton et al., 1993; Janz et al., 1998). Furthermore, SV2 interacts *in vitro* with synaptotagmin, the Ca^{2+} sensor for exocytosis (Fernández-Chacón et al., 2001; Sun et al., 2007), suggesting that SV2 acts by binding to synaptotagmin (Schivell et al., 1996), although the mode of interaction remains unclear (Pyle et al., 2000; Lazzell et al., 2004; Schivell et al., 2005). SV2C is the protein receptor for botulinum neurotoxin A, which blocks neurotransmitter release by cleaving SNAP-25 (Dong et al., 2006;

Received Sept. 21, 2008; revised Nov. 21, 2008; accepted Nov. 26, 2008.

This work was supported by the Howard Hughes Medical Institute. We thank Drs. A. Maximov, P. Kaeser, and F. Deak for advice and I. Kornblum and A. Roth for outstanding technical assistance.

Correspondence should be addressed to Thomas C. Südhof at his present address: Neuroscience Institute, Department of Molecular and Cellular Physiology, and Howard Hughes Medical Institute, Stanford University School of Medicine, Palo Alto, CA 94304-5543. E-mail: tcs1@stanford.edu.

DOI:10.1523/JNEUROSCI.4521-08.2009

Copyright © 2009 Society for Neuroscience 0270-6474/09/290883-15\$15.00/0

Mahrhold et al., 2006). Finally, SV2 is the target of the anti-epileptic drug levetiracetam (Lynch et al., 2004).

SV2B KO mice are phenotypically normal, whereas SV2A KO mice (and SV2A/SV2B double-KO mice) exhibit severe seizures and die postnatally, without developmental changes in brain structure (Janz et al., 1999). Electrophysiologically, cultured hippocampal SV2A- or SV2B-deficient neurons exhibit no detectable abnormalities. In contrast, neurons lacking both isoforms display sustained synaptic facilitation during high-frequency stimulus trains that is reversed by a membrane-permeable EGTA analog that chelates intracellular free Ca^{2+} (Janz et al., 1999). Thus, synaptic facilitation caused by accumulating residual Ca^{2+} during the high-frequency stimulus trains is enhanced in SV2-deficient synapses (Janz et al., 1999). Moreover, in SV2A-deficient mice, acute slices exhibit abnormal GABAergic synaptic transmission, the size of the pool of release-ready chromaffin secretory vesicles is decreased, and SNARE-complex assembly in brain may be impaired, suggesting that SV2A may function upstream of Ca^{2+} triggering in priming synaptic vesicles (Crowder et al., 1999; Xu and Bajjalieh, 2001). These results were supported by studies in cultured hippocampal neurons suggesting that SV2 primes vesicles in quiescent neurons, and that this function can be bypassed by an activity-dependent priming mechanism (Custer et al., 2006).

Although the currently available data thus establish that SV2 is important for neurotransmitter release, they do not clarify at what step during exocytosis SV2 functions. Whereas the binding of SV2 to synaptotagmin indicates a role in Ca^{2+} triggering, other experiments suggested a function in vesicle priming, possibly in an activity-dependent manner as indicated by the synaptic facilitation. Moreover, it is unknown how the physiological role of SV2 relates to its intravesicular glycosylation and its transporter-like structure. In the present study, we have investigated these issues using an electrophysiological analysis of SV2-deficient cultured neurons, either without further treatment or after rescue with wild-type or mutant SV2A delivered by lentiviral infection. Our results indicate that SV2 acts as a booster of synaptic exocytosis upstream of Ca^{2+} triggering, but downstream of priming, in a function that is independent of its possible binding to synaptotagmin, but requires a normal transmembrane structure and intravesicular glycosylation.

Materials and Methods

Plasmid construction. The wild-type rat SV2A cDNA was replicated by PCR and cloned into pFUW lentivirus expression vector (with multiple cloning sites: *Xba*I, *Eco*RI, *Bst*BI, *Nhe*I, *Bam*HI, and *Hpa*I) using *Eco*RI and *Bam*HI. EGFP was inserted in frame at the N terminus of SV2A between the *Xba*I and *Eco*RI sites. Mutations were generated by PCR and subcloned into pFUGW (G = EGFP) vector. DA mutant contains alterations of an aspartic acid to alanine at 179 aa and a glutamic acid to alanine at 182 aa. NQ mutant contains three asparagine-to-glutamine mutations at 498 aa, 548 aa, and 573 aa on glycosylated residues. KA mutant includes a lysine to alanine mutation at 694 aa. Mutant d107 was generated by deleting first 107 aa residues, which was denoted as the N-terminal synaptotagmin binding region of SV2A (Schivell et al., 1996; Lazzell et al., 2004; Schivell et al., 2005). Sequences are verified by DNA sequencing.

Mouse breedings. All analyses were performed on littermate offspring of breedings between SV2A heterozygotes/SV2B knock-out (KO) homozygotes [SV2A(+/-)/SV2B(-/-)]. Cultured cortical neurons from SV2A wild-type/SV2B homozygous [SV2A(+/+)/SV2B(-/-)] pups and SV2A/SV2B homozygous [SV2A(-/-)/SV2B(-/-)] pups were used in the experiments in this study. All genotyping was performed as described previously (Janz et al., 1999), except primers A1* (GAGT-TAGGGATGAGTGTCTGG), A2* (GTTGACTGAGAGTGAGAT-

GAGC), and N (GAGCGCGCGGGCGGAGTTGTTGAC) were used for SV2A.

Cortical primary neuronal cultures. The cortexes were dissected from the brains of postnatal day 1 (P1) mice, dissociated by trypsin digestion, and plated on circle glass coverslips coated with Matrigel. The cortical neurons were maintained in MEM medium (Invitrogen) supplemented with B-27 (Invitrogen), L-glutamine, 0.5% glucose, 5% fetal bovine serum, and Ara-C (Sigma-Aldrich). The cultures were used for experiments at 14–17 DIV. For the tests of the effect of neuronal silencing on the SV2 KO phenotype, we incubated the cultured neurons for 24 h in the regular medium containing 1 μ M tetrodotoxin (TTX) before performing the analyses.

Electrophysiology. Synaptic responses were triggered by 1 ms current injection (900 μ A) through a local extracellular electrode (FHC concentric bipolar electrode; catalog #CBAEC75) and recorded in whole-cell mode using Multiclamp 700A amplifier (Molecular Devices). Model 2100 Isolated Pulse Stimulator (A-M Systems) was used to control the frequency, duration, and magnitude of extracellular stimulus. The whole-cell pipette solution contained 135 mM CsCl₂, 10 mM HEPES, 1 mM EGTA, 1 mM Na-GTP, 4 mM Mg-ATP, and 10 mM QX-314, pH 7.4. The bath solution contained 140 mM NaCl, 5 mM KCl, 2 mM MgCl₂, 10 mM HEPES-NaOH, pH 7.4, 10 mM glucose, and 1 mM Ca²⁺ if not indicated otherwise. Signals were digitized at 10 kHz, filtered at 2 kHz, and stored using pClamp9 (Axon Instruments) software. Spontaneous synaptic responses (mIPSCs and mEPSCs) were monitored in the presence of 1 μ M TTX to block action potentials. Spontaneous mEPSCs were recorded with additional 100 μ M picrotoxin in the bath solution. IPSCs were pharmacologically isolated by adding 50 μ M APV and 20 μ M CNQX to suppress the excitatory AMPA and NMDA currents. Synaptic responses were recorded at least 1 min after obtaining whole-cell patch before recording of evoked synaptic responses, allowing the internal pipette solution to diffuse into the patched neuron. Series resistance was compensated to 60–70%. For EGTA-AM [EGTA-tetra (acetoxymethyl ester)] experiments, cultured neurons were pretreated with EGTA-AM at 0.1 mM for at least 10 min. Hypertonic sucrose (0.5 M) was applied for 30 s, or 20 s for the tests of the effect of neuronal silencing on the SV2 KO phenotype, through perfusion system at speed of 1 ml/min. All experiments were performed at room temperature. Ionomycin was applied with a puff pipette at 5 μ M in the presence of 50 μ M APV and 20 μ M CNQX. The synaptic charge transfer induced by the ionomycin was integrated from for 1.5 min, and the time to peak was measured from time of adding ionomycin to the peak of response. The recovery rates of synapses were measured at 0.1 Hz immediately after applying 100 stimuli of 10 Hz. Data were analyzed using Clampfit 9.0 (Molecular Devices). mIPSC and mEPSC event detections were performed manually to collect individual mIPSCs and mEPSCs. Statistical analysis was performed with *t* test (**p* ≤ 0.05, ***p* ≤ 0.01, and ****p* ≤ 0.001). All data are shown as means ± SEMs. Cortical neurons were infected with lentiviruses encoding EGFP fusion proteins of wild-type or mutant SV2A as indicated. The cultures were infected before 7 DIV and analyzed at 14–17 DIV. As determined by EGFP fluorescence, the efficiency of lentiviral infections exceeded 95%; therefore, we randomly selected the neurons for whole-cell recording assuming that most presynaptic inputs in infected cultures were formed by neurons expressing recombinant protein of interest.

Immunocytochemistry. Neurons attached to the glass coverslips were rinsed once with PBS, fixed for 15 min on ice in 4% of formaldehyde and 4% of sucrose in PBS. After fixation, the neurons were washed with PBS twice, and then incubated for 30 min in blocking solution, PBSS, containing 3% milk, 0.1% saponin, and in PBS, followed by 1 h incubation with primary and rhodamine- and FITC-conjugated secondary antibodies diluted in blocking solution. The coverslips were then mounted on glass slides with Aqua-Poly/Mount medium (Polysciences) and analyzed at room temperature using a confocal microscope (DMIRE2; Leica) and 63×/1.32–0.6 oil-immersion objective. The images were collected using confocal software (Leica) and processed using Photoshop software (Adobe). All digital manipulations were equally applied to the entire image.

Miscellaneous. Samples of EGFP-SV2 recombinant proteins were collected by adding 1× sample buffer (Laemmli, 1970) to cultured cortical

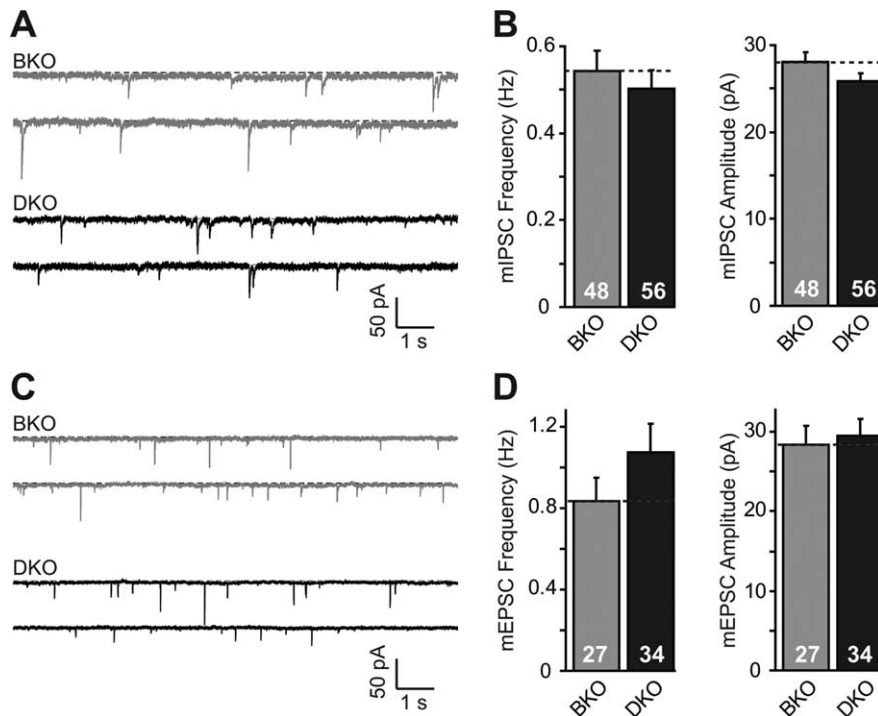


Figure 1. Spontaneous synaptic transmission is not altered in SV2-deficient neurons. **A–D**, Representative traces (**A**, **C**) and the frequency and amplitude (**B**, **D**) of mIPSCs (**A**, **B**) and mEPSCs (**C**, **D**) recorded in neurons from SV2B KO mice (BKO) or from SV2A/SV2B double-KO mice (DKO). Spontaneous events were recorded in a bath solution containing 2 mM Ca^{2+} and 0.5 mM Mg^{2+} at a -70 mV holding potential in the presence of 1 μM TTX and 20 μM CNQX/50 μM APV (for mIPSCs) or 100 μM picrotoxin (for mEPSCs). All data shown are means \pm SEMs (n = numbers shown in bar diagrams from at least 3 independent cultures). Note that the numerical values for all electrophysiological data are listed in supplemental Table 1 (available at www.jneurosci.org as supplemental material).

neurons, boiled for 10 min, then stored at -80°C until used. Samples were analyzed by SDS-PAGE and electroblotted to nitrocellulose membranes (Amersham). The membranes were probed using antibodies against SV2A (P915), EGFP (JL-8, Clontech), and GDI (CL81.2). SDS-PAGE and immunoblotting were performed as standard procedure described (Laemmli, 1970; Janz et al., 1999).

Results

Analysis of the effect of deleting SV2 on inhibitory and excitatory synaptic transmission

We prepared high-density cultures of cortical neurons from double-KO mice that lack both SV2A and SV2B, and from littermate control mice that lack only SV2B but contain at least one wild-type allele of SV2A (Janz et al., 1999). The cultured neurons were analyzed electrophysiologically using postsynaptic whole-cell recordings as described previously (Maximov et al., 2007). Spontaneous miniature and evoked IPSCs (mIPSCs and IPSCs, respectively) were recorded in the presence of AMPA- and NMDA-receptor blockers (20 μM CNQX and 50 μM AP-5), whereas spontaneous miniature and evoked EPSCs (mEPSCs and EPSCs, respectively) were monitored in the presence of the GABA-receptor blocker picrotoxin (100 μM). SV2B KO neurons were used as a control for SV2A/2B double-KO neurons because previous studies showed that SV2B-deficient mice exhibit no detectable phenotype compared with wild-type controls, whereas SV2A/2B double-KO neurons exhibit a significant phenotype (Janz et al., 1999). To confirm this previous result and to ensure that this lack of an obvious phenotype in SV2B KO mice, initially described for autapses formed by isolated cultured hippocampal neurons, also applies to synapses formed between cortical neurons cultured at high density, we compared the salient physiolog-

ical properties of cortical neurons cultured from littermate wild-type and SV2B KO mice. We detected no difference, confirming that the SV2B KO by itself does not produce a major phenotype and can thus be used as a control (supplemental Fig. 1, available at www.jneurosci.org as supplemental material).

We first examined action potential-independent, spontaneous “miniature” neurotransmitter release events in the presence of 1 μM TTX. Consistent with the results of Custer et al. (2006), the frequency and amplitude of spontaneous mIPSCs and mEPSCs were not significantly different between synapses lacking either only SV2B or both SV2A and SV2B, although the mEPSC frequency in the double-KO neurons tended to be slightly higher (Fig. 1*A–D*).

We next investigated whether deletion of SV2A and SV2B impaired evoked IPSCs (Fig. 2*A*). In these experiments, IPSCs were measured instead of EPSCs because in our recording system, IPSCs can be more accurately and reliably monitored than EPSCs (Maximov et al., 2007). We detected a highly significant ~ 30 – 40% decrease in the peak amplitudes and the synaptic charge transfer (integrated over 1.5 s) of IPSCs in neurons lacking SV2A and SV2B compared with control neurons lacking only SV2B (Fig. 2*B*). Kinetic analyses did not uncover a difference in the IPSC kinetics between SV2A/2B double-KO and SV2B single-KO neurons, indicating that the change in release is not due to a selective loss of synchronous or asynchronous release (data not shown).

The observation that the SV2 double-KO decreases action-potential-evoked release (Fig. 2*B*) and binds to synaptotagmin (Schivell et al., 1996) suggests that SV2 may act during Ca^{2+} triggering of release mediated by synaptotagmin, and may alter the Ca^{2+} affinity of release. To test this hypothesis, we measured the amplitude of IPSCs evoked in the presence of different concentration of extracellular Ca^{2+} . Plots of the absolute IPSC amplitudes showed that at all except the lowest Ca^{2+} concentration, synapses lacking SV2 proteins exhibited a uniform ~ 30 – 40% decrease in the peak amplitude (Fig. 2*C*). This relationship indicates that the SV2 deletion does not alter the apparent Ca^{2+} affinity of release, as confirmed by plots of the normalized IPSC amplitudes, which revealed an identical Ca^{2+} concentration dependence of release in SV2-deficient and control synapses (Fig. 2*D*).

Deletion of SV2 does not decrease the readily releasable pool size

To determine whether the decrease in inhibitory neurotransmitter release in SV2-deficient neurons is due to a decrease in the readily releasable pool (RRP) of primed vesicles, we applied hypertonic sucrose to cultured neurons for 30 s and estimated the size of the RRP as the integrated charge transfer over the first 10 s (Fig. 2*E*). Hypertonic sucrose is thought to stimulate release of the entire RRP in cultured neurons, thereby allowing measurement of the RRP (Rosenmund and Stevens, 1997). Surprisingly,

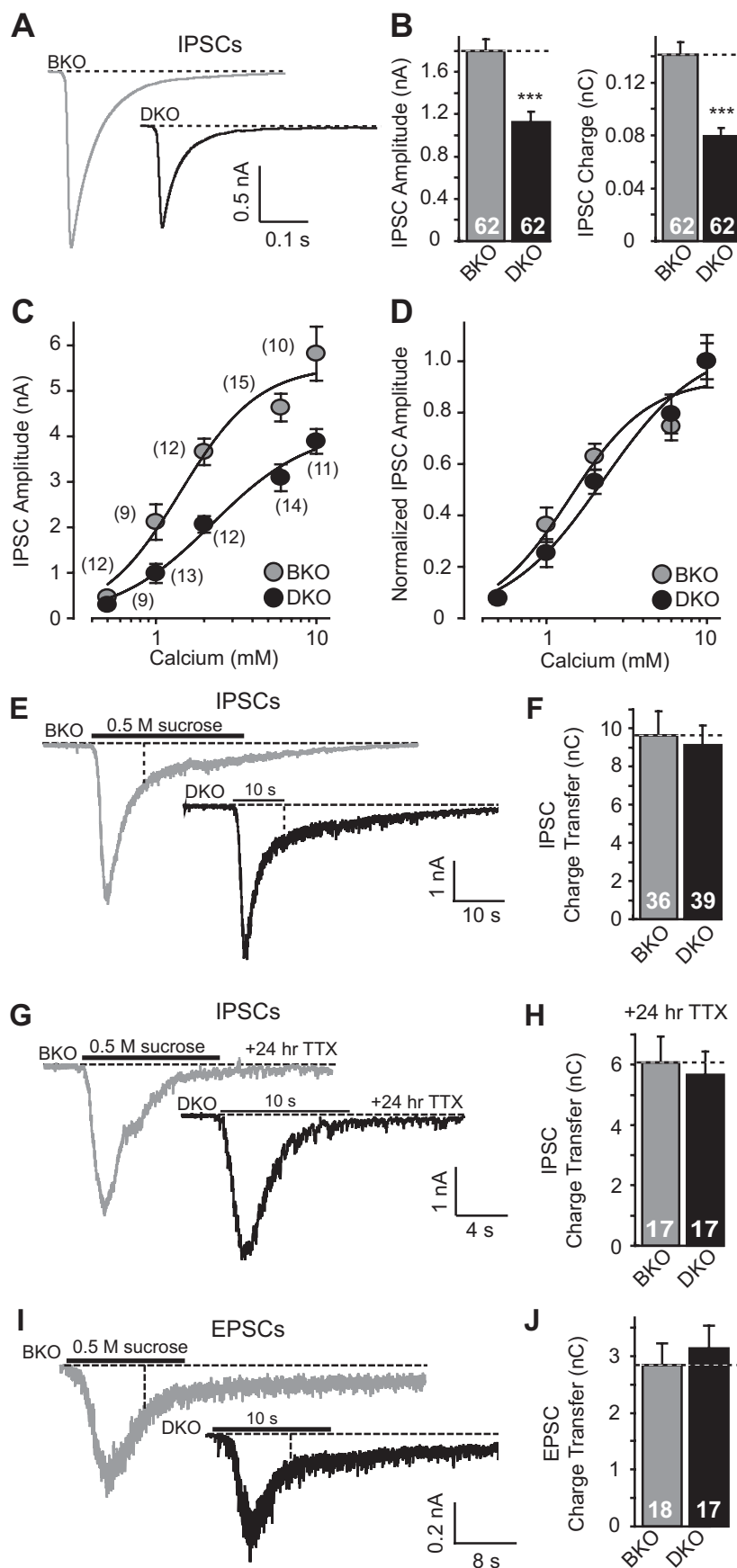


Figure 2. SV2 deletion selectively impairs Ca^{2+} triggering of release without decreasing the RRP. **A, B**, Representative traces (**A**) and mean amplitude and charge transfer (**B**) of IPSCs evoked by extracellular stimulation at 0.1 Hz frequency in cultured cortical neurons from littermate SV2BKO (BKO) and SV2A/SV2B double-KO mice (DKO). Action potentials were evoked with a focal

electrode in a bath solution containing 1 mM Ca^{2+} and 2 mM Mg^{2+} . **C, D**, Ca^{2+} titration of IPSC amplitudes in BKO and DKO neurons plotted in absolute terms (**C**) or normalized to the maximal Ca^{2+} concentration (**D**). Recordings were performed in bath solutions containing the indicated Ca^{2+} concentrations with a constant 2 mM Mg^{2+} concentration. **E–J**, Measurements of the RRP size by application of 0.5 M sucrose in either inhibitory (**E–H**) or excitatory (**I, J**) synapses in cultured neurons that were either not treated (**E, F, I, J**) or treated with 1 μM TTX for 24 h (**G, H**). Panels show representative traces (**E, G, I**) and summary graphs depicting the integrated charge transfer during the first 10 s of the response (**F, H, J**). All data shown are means \pm SEMs (n = numbers shown in bar diagrams from at least 3 independent cultures; *** p < 0.001 by Student's t test; in **C** and **D**, n = numbers shown above or under data points; the absolute values are significantly different between BKO and DKO neurons at the p < 0.0001 level as tested by 2-way ANOVA).

Release induced with the Ca^{2+} ionophore ionomycin

The phenotype we observe in the SV2-deficient synapses is puzzling: a decrease in evoked responses induced by isolated action potentials without a change in mini frequency, mini amplitude, apparent Ca^{2+} sensitivity of release, or the size of the RRP. This result suggests that there is either an intrinsic methodological problem with the data we obtained since the results do not fit into any standard scheme of synaptic vesicle exocytosis (i.e., a decrease in release probability should be ac-

←

electrode in a bath solution containing 1 mM Ca^{2+} and 2 mM Mg^{2+} . **C, D**, Ca^{2+} titration of IPSC amplitudes in BKO and DKO neurons plotted in absolute terms (**C**) or normalized to the maximal Ca^{2+} concentration (**D**). Recordings were performed in bath solutions containing the indicated Ca^{2+} concentrations with a constant 2 mM Mg^{2+} concentration. **E–J**, Measurements of the RRP size by application of 0.5 M sucrose in either inhibitory (**E–H**) or excitatory (**I, J**) synapses in cultured neurons that were either not treated (**E, F, I, J**) or treated with 1 μM TTX for 24 h (**G, H**). Panels show representative traces (**E, G, I**) and summary graphs depicting the integrated charge transfer during the first 10 s of the response (**F, H, J**). All data shown are means \pm SEMs (n = numbers shown in bar diagrams from at least 3 independent cultures; *** p < 0.001 by Student's t test; in **C** and **D**, n = numbers shown above or under data points; the absolute values are significantly different between BKO and DKO neurons at the p < 0.0001 level as tested by 2-way ANOVA).

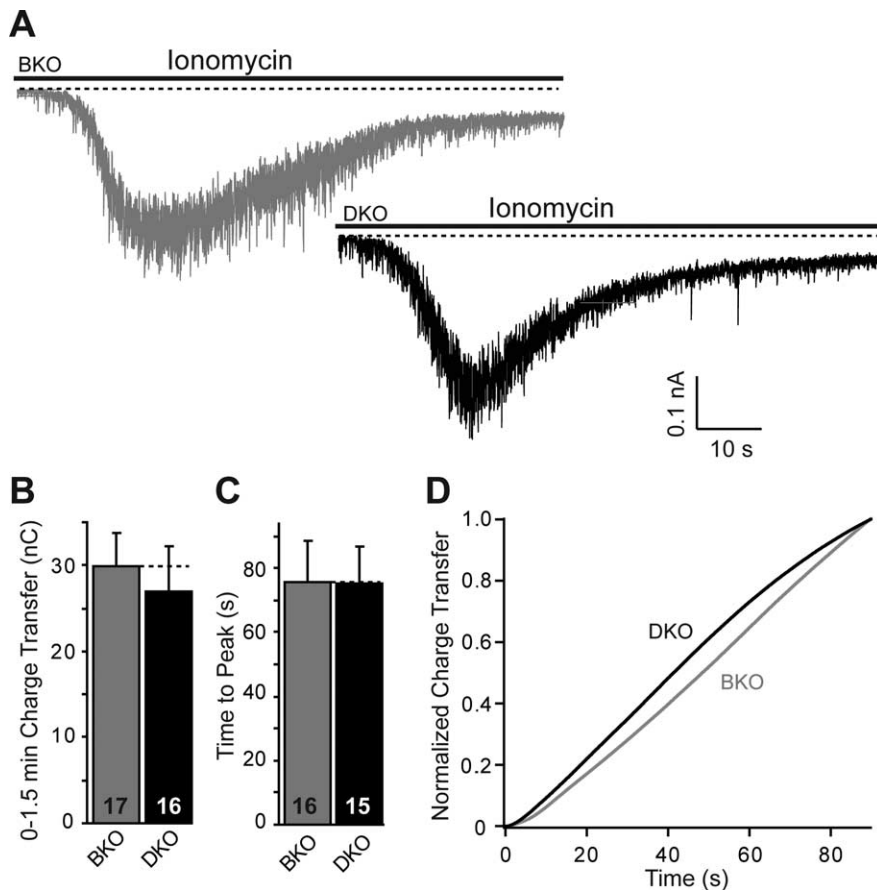


Figure 3. Effect of ionomycin on release in SV2B KO and SV2A/SV2B double-KO synapses. *A*, Representative IPSC traces triggered by application of $5 \mu\text{M}$ ionomycin in SV2B KO (BKO) and SV2A/SV2B double-KO (DKO) neurons in 1 mM Ca^{2+} . Excitatory currents were blocked by APV and CNQX. The scale bar applies to both traces. *B*, *C*, Total synaptic charge transfer for ionomycin-induced responses (*B*) and average delays from the point of application of ionomycin to maximum amplitude of inhibitory response (*C*) in SV2B-deficient and SV2A/SV2B double-deficient neurons. Data shown are means \pm SEMs (n = numbers shown in bar diagrams from 2 independent cultures). *D*, Normalized cumulative charge as a function of time to illustrate the kinetics of ionomycin-induced release in SV2B KO (BKO) and SV2A/SV2B double-KO (DKO) synapses.

companied either by a decrease in RRP or in Ca^{2+} sensitivity of a synapse) or that the standard scheme of synaptic vesicle exocytosis is incomplete and SV2 functions in a novel facilitatory step between priming and Ca^{2+} triggering. Other alternative explanations would be that the SV2 deletion decreases the transmitter filling of synaptic vesicles, or that it impairs action potential generation. However, these last two alternatives appear unlikely given the normal mini amplitude, which argues against a filling defect, and the synaptic vesicle localization of SV2, which argues against a role in activating plasma-membrane channels.

To ensure that the results obtained by the application of hypertonic sucrose are correct, we used an independent method to trigger exocytosis of the entire RRP, namely application of the Ca^{2+} ionophore ionomycin (Maximov and Südhof, 2005). This method not only provides an estimate of the Ca^{2+} -stimulatable RRP size, but also allows a crude measurement of the Ca^{2+} sensitivity of release since the kinetics of release induced by ionomycin reflects the time course of the intraterminal Ca^{2+} increase. Using this approach, we detected no difference between synapses lacking only SV2B or both SV2A and SV2B in the size of the ionomycin-releasable RRP or the kinetics of ionomycin-induced release (Fig. 3). These results support the notion that SV2 acts at a novel step in synaptic vesicle exocytosis that renders primed vesicles Ca^{2+} responsive.

Synaptic responses to a 10 Hz stimulus train in SV2-deficient neurons

To test the role of SV2 in Ca^{2+} -triggered release evoked by a high-frequency stimulus train, we evoked IPSCs by 10 action potentials applied at 10 Hz in 1 mM Ca^{2+} and 2 mM Mg^{2+} (Fig. 4*A*). Measurements of the amount of total release during the train (“train release”), after the train (“delayed release”), or both (“total charge transfer”) were obtained by integrating the synaptic charge transfer over the respective time periods. Train release was calculated by integrating the synaptic transfer charge from the beginning of the train until 0.1 s after last stimulus; total charge transfer was calculated by integrating over 5 s of the train (i.e., it includes all release); and delayed release is the difference between total charge transfer and train release. These measurements revealed the same $\sim 40\%$ decrease in all parameters of release in SV2-deficient synapses compared with control synapses as detected for isolated IPSCs (Fig. 4*B–D*). All measures of release induced by the 10 Hz stimulus train (train release, delayed release, total charge transfer) were decreased similarly. Much of the release during the train, and all of it during the “delayed release” period after the train, is asynchronous, whereas release induced by isolated action potentials is largely synchronous (Maximov and Südhof, 2005). Thus, as observed for IPSCs triggered by isolated action potentials, deletion of SV2 equally impairs synchronous and asynchronous release. Note that this

high-frequency stimulation paradigm is not saturating, and thus the release observed does not correspond to the size of the RRP, which we have shown above is unchanged in the SV2 DKO.

We next plotted the synchronous components of release during the 10 Hz stimulus train as normalized responses as a function of the stimulus number (Fig. 4*E*). In control neurons lacking only SV2B, the 10 Hz stimulus train induced a progressive reduction in synaptic responses (referred to as short-term synaptic depression). In SV2-deficient neurons, however, the 10 Hz stimulus train induced an increase in synaptic responses (i.e., synaptic facilitation) (Fig. 4*E*). Since the relative decrease in the total amount of release during a stimulus train and an isolated action potential induced by the SV2 deletion are similar, the facilitation of synchronous responses observed in SV2-deficient synapses likely represents a Ca^{2+} -dependent shift from asynchronous to synchronous release during the stimulus train. This behavior is consistent with the notion that with an unchanged RRP but decreased ability of Ca^{2+} to trigger release, the accumulating Ca^{2+} during the stimulus train causes facilitation of synaptic responses in the SV2A/2B double-KO neurons since the RRP does not become depleted.

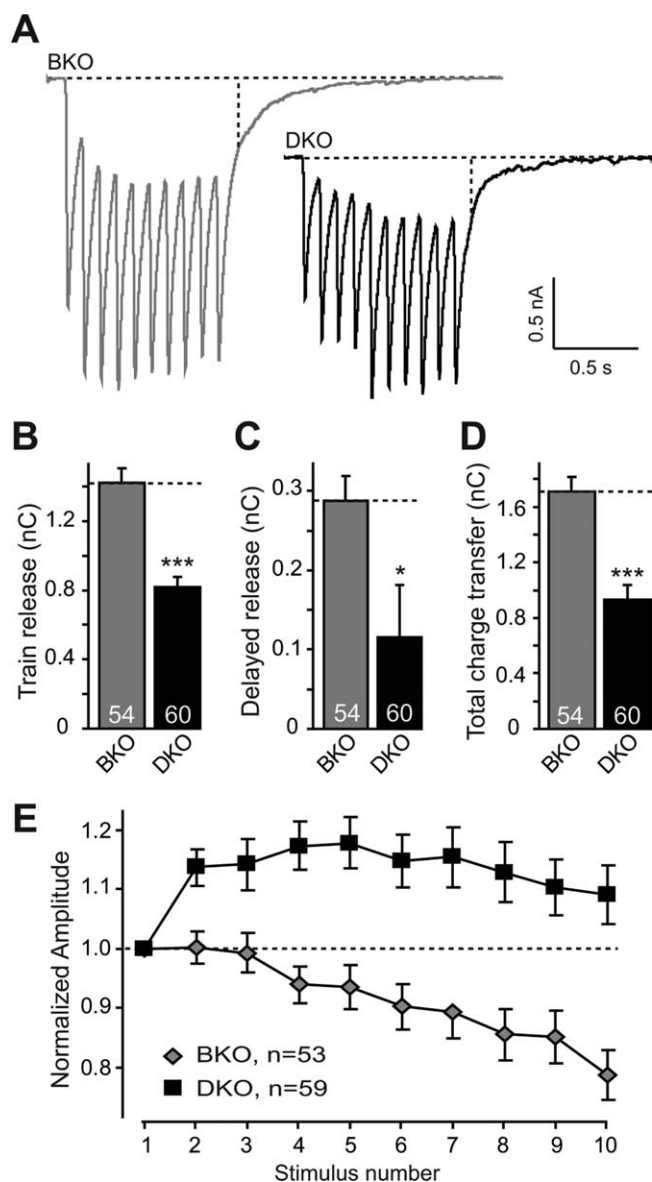


Figure 4. SV2 deletion decreases release but increases facilitation during 10 Hz stimulus trains. **A**, Representative traces of IPSCs induced by a 1 s, 10 Hz stimulus train in cultured neurons from SV2B KO (BKO) and SV2A/SV2B double-KO (DKO) mice (bath solution contains 1 mM Ca^{2+} and 2 mM Mg^{2+}). **B–D**, Summary graphs of the charge transfer during the stimulus train (train release, **B**), after the train (delayed release, **C**, a measure of asynchronous release), and over the entire experiment (total charge transfer, **D**) in BKO and DKO neurons. **E**, Plot of the normalized amplitude as a function of the stimulus number during the 10 Hz stimulus train. As amplitudes, only the synchronous component of the response is measured. All data shown are means \pm SEMs (n = numbers shown in bar diagrams from at least 3 independent cultures; * p < 0.05, ** p < 0.01, and *** p < 0.001 by Student's *t* test; in **E**, n = 53 for BKO neurons and n = 59 for DKO neurons; values are significantly different between BKO and DKO neurons at the p < 0.0001 level as tested by 2-way ANOVA).

EGTA-AM reverses facilitation induced by deletion of SV2 but does not abolish phenotype

We previously hypothesized that SV2 functions as a Ca^{2+} uptake system that clears Ca^{2+} from nerve terminals after a pulse of Ca^{2+} has entered the terminals during an action potential (Janz et al., 1999). This hypothesis was based on the observation that the synaptic facilitation phenotype in SV2-deficient synapses was reversed by EGTA-AM, which sequesters intracellular Ca^{2+} . However, the decrease in total release observed in the current study [which we could not measure in our previous study due to

technical limitations (Janz et al., 1999)] strongly argues against this hypothesis because an impairment in Ca^{2+} uptake into synaptic vesicles should not lead to a decrease in the synaptic response during an isolated action potential or stimulus train. To confirm this, we tested the effect of EGTA-AM on release induced by isolated action potentials (Fig. 5A–C) or action potential trains (Fig. 5D–G). We pretreated cultured neurons with EGTA-AM for at least 10 min before recording synaptic responses. EGTA-AM treatment suppressed release in SV2-deficient and control synapses to an almost identical relative amount (Fig. 5B), even though the absolute amount of release was decreased ~40% in the SV2-deficient synapses. This observation was true for release induced by isolated action potentials (~60% EGTA-induced decrease), and for release induced by action potential trains (~70% EGTA-induced decrease).

However, when we examined synaptic facilitation/depression during the 10 Hz stimulus train, we found that EGTA-AM reversed the facilitation in SV2-deficient synapses, which now became depressing synapses indistinguishable from control synapses (Fig. 5H). This observation confirms our earlier result (Janz et al., 1999), suggesting that EGTA-AM selectively reverses the short-term synaptic plasticity phenotype induced by deletion of SV2, even though it does not rescue the decrease in release induced by the deletion. Viewed together with the data in Figure 3, these results suggest that the synaptic facilitation of synaptic responses during the 10 Hz stimulus train in SV2-deficient synapses is due to accumulating Ca^{2+} triggering a larger remaining RRP.

To test for other potential changes in vesicle dynamics in SV2-deficient synapses, we measured the speed with which synaptic responses recover after synaptic depression was induced by a high-frequency stimulus train. The stimulus train depletes the RRP, and the recovery rate of synaptic responses thus measures the rate of RRP refilling. We monitored IPSCs in SV2-deficient and control neurons at a 0.1 Hz stimulation frequency to establish a stable baseline, then applied a 10 s/10 Hz to deplete the RRP as manifested by synaptic depression, and afterward monitored the recovery of IPSCs again at a 0.1 Hz stimulus frequency (Fig. 6A). We plotted the results both as absolute amplitudes to display the decrease in synaptic responses observed in the SV2-deficient synapses (Fig. 6B), and as normalized synaptic responses to analyze the recovery kinetics (Fig. 6C). This experiment clearly confirmed the decrease in synaptic strength induced by deletion of SV2 (Fig. 6B), but failed to uncover any change in recovery kinetics in SV-deficient synapses (Fig. 6C). Thus, deletion of SV2 does not affect the size or the dynamics of the RRP.

The SV2 KO phenotype can be rescued by viral expression of wild-type SV2

To investigate whether the phenotype of SV2-deficient synapses may reflect a developmental change or is related to an acute action of SV2 in synaptic transmission, we tested whether the phenotype could be rescued by expression of wild-type SV2A in SV2-deficient neurons. We produced lentivirus expressing an EGFP fusion protein of rat SV2A, and infected SV2-deficient neurons with this lentivirus within 7 d *in vitro* (DIV). The neurons were then analyzed at 14–17 DIV.

Fluorescence microscopy revealed that the exogenous EGFP-fusion protein of SV2 was expressed in a punctate pattern, consistent with a synaptic localization (Fig. 7A). Measurements of synaptic responses induced by isolated action potentials (Fig. 7B–D) or 10 Hz stimulus trains (Fig. 7E–I) demonstrated that the SV2 EGFP-fusion protein rescued all aspects of the SV2-

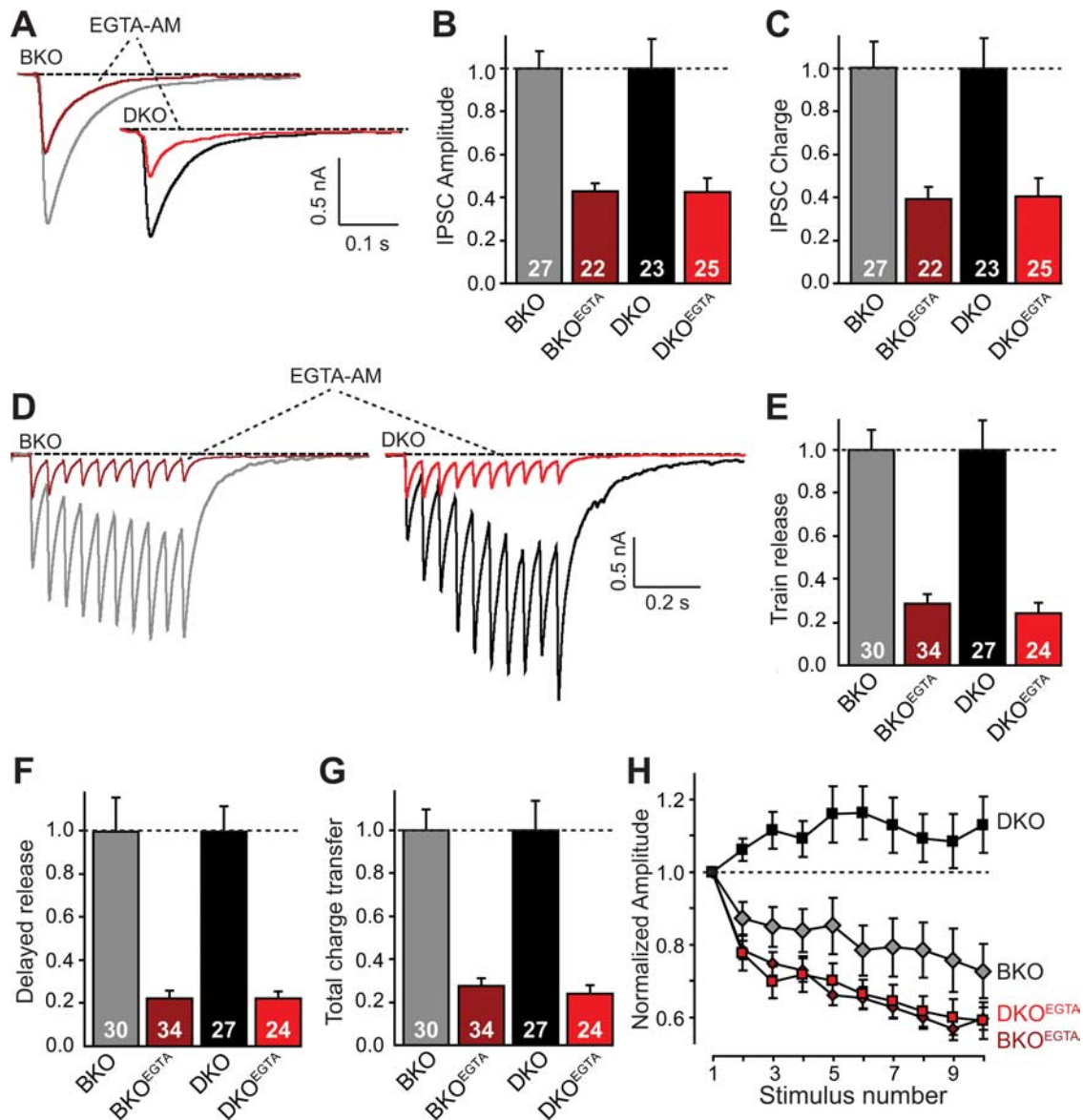


Figure 5. Effect of EGTA-AM on synaptic responses in SV2-deficient neurons. **A–C**, Representative traces (**A**) and summary graphs of the amplitudes (**B**) and synaptic charge transfers (**C**) of evoked IPSCs in neurons from SV2B KO mice (BKO) and SV2A/B double-KO mice (DKO), recorded before or after pretreatment with 0.1 mM EGTA-AM (>10 min). Data are normalized for the response before the EGTA-AM treatment; no statistically significant difference in the relative effect of EGTA-AM on the response size was detected. **D–G**, Effect of EGTA-AM on synaptic responses evoked during a 10 Hz stimulus train (1 s). Data shown are representative traces (**D**) and summary graphs of the train release (**E**), the delayed release (**F**), and the total release (**G**). In **E–G**, responses are normalized for the naive condition. **H**, Effect of EGTA-AM on the facilitation induced by deletion of SV2. The graph depicts a plot of the relative amplitude of synaptic responses as a function of the stimulus number during a 10 Hz stimulus train observed in BKO and DKO neurons. As amplitudes, only the synchronous components of the responses are measured. All data shown are means \pm SEMs (n = numbers shown in bar diagrams from at least 3 independent cultures; the effect of EGTA-AM is not statistically significantly different between neurons from BKO and DKO mice; in **H**, n = 29 for BKO synapses; n = 33 for BKO synapses treated with EGTA-AM; n = 26 for DKO synapses; and n = 25 for DKO synapses treated with EGTA-AM; values are significantly different between naive and EGTA-AM-treated neurons from DKO mice at the $p < 0.0001$ level as tested by 2-way ANOVA, whereas the responses from BKO versus DKO mice are not significantly different after EGTA-AM treatment).

deficiency phenotype, i.e., both the release and the short-term plasticity impairments. Thus, the EGFP-SV2 fusion protein introduced into the neurons after synapse development had been initiated was clearly fully functional, suggesting that SV2 acts acutely during release.

Structure–function analysis of SV2

Since lentivirally expressed SV2A rescues the electrophysiological SV2 deficiency phenotype, we are now in a position to investigate the structure–function relations of SV2. We used four mutations in conserved sequences that were previously implicated in functional hypotheses about SV2 action (Fig. 8A).

First, we deleted in “SV2A^{d107}” 107 N-terminal residues

that include the conserved cytoplasmic sequence that binds to synaptotagmin (Schivell et al., 1996 and 2005; however, see Lazzell et al., 2004 for an alternative view), and coincidentally includes the epitope for the canonical SV2 antibody (Bajjalieh et al., 1992).

Second, we substituted in “SV2A^{KA}” a highly conserved lysine residue in the fifth cytoplasmic loop of SV2 (lysine 694) for alanine.

Third, we substituted in “SV2A^{DA}” two conserved charged residues in TMR1 that are also present in SVOP (aspartate 179 and glutamate 182) (Janz et al., 1999) for alanines.

Fourth, we substituted in “SV2A^{NQ}” three asparagines that represent the conserved N-glycosylation sites in the large intra-

vesicular loop of SV2 for glutamines (asparagine 498, asparagine 548, and asparagine 573).

All of these mutants were analyzed as EGFP-fusion proteins since EGFP-fused wild-type SV2A fully rescued the KO phenotype (Fig. 7). The EGFP allowed us to directly visualize the localization of the expressed protein.

Initial tests of the expression of the various SV2 mutants in cultured neurons confirmed that all of them were produced at the expected molecular weight (Fig. 8*B,C*). However, the relative expression levels of the mutants in which the glycosylation site (SV2A^{NQ}) or the charged residues in TMR1 were substituted (SV2A^{DA}) were very low compared with wild-type SV2A or the other two mutant SV2A variants. This observation suggests that the mutations in the glycosylation site and in TMR1 may potentially destabilize the protein.

The N-terminal synaptotagmin-binding sequence is not essential for SV2 function

We first focused on our observation that SV2 is required for Ca²⁺ triggering of vesicle exocytosis without being essential for normal priming of vesicles, which suggests an action for SV2 coincident with that of synaptotagmin, the Ca²⁺ sensor for release. Since SV2A was reported to directly bind to synaptotagmin via a conserved N-terminal sequence (Schivell et al., 1996, 2005), we tested whether this N-terminal sequence was in fact essential for rescue. We found that mutant SV2A lacking its N-terminal 107 residues (referred to as the d107 mutant) was localized to a punctate “synaptic” pattern in cultured SV2-deficient neurons (Fig. 9*A*), and was fully capable of reversing the SV2 deficiency phenotype, including the decrease in release evoked by single action potentials (Fig. 9*B,C*) and by 10 Hz stimulus trains (Fig. 9*D–G*). These findings indicate that binding of the N-terminal conserved SV2 sequence to synaptotagmin is not essential for its function.

Lysine 694 is dispensable for SV2 function

We next investigated the lysine 694 residue in SV2A that we mutated to alanine (referred to as the KA mutation). Lysine 694 is located N-terminal to the 11th TMR and is conserved in all SV2 isoforms (Fig. 8*A*). Again, the KA mutation did not abolish rescue, i.e., had no effect on either the localization of SV2A or its ability to restore normal release elicited by isolated action potentials, or 10 Hz stimulus trains of action potentials (supplemental Fig. 2, available at www.jneurosci.org as supplemental material). Moreover, the short-term plasticity phenotype of the SV2 deletion was also fully rescued.

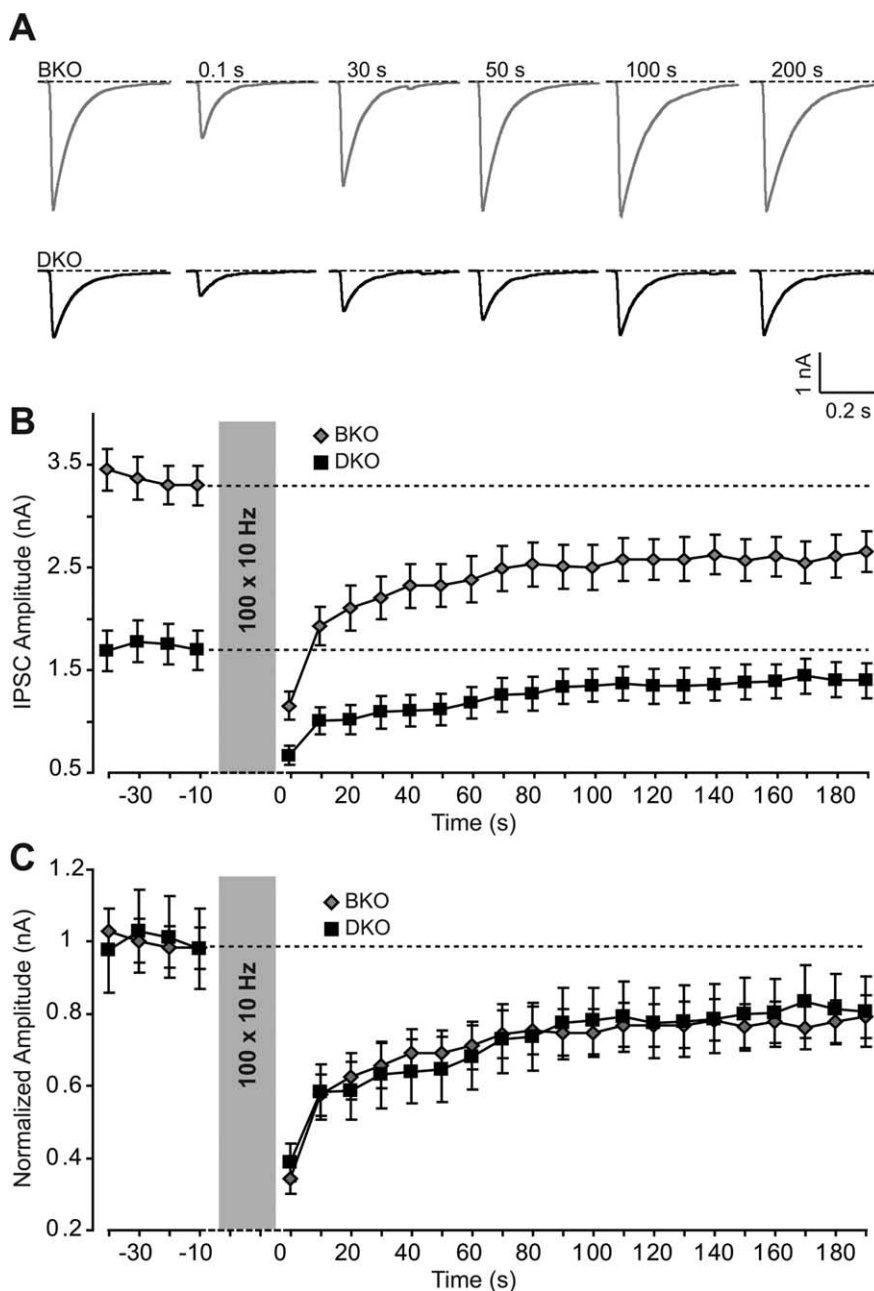


Figure 6. Recovery of synaptic responses in SV2B KO and SV2A/SV2B double-KO synapses after use-dependent depression induced by high-frequency stimulation. *A*, Representative traces of IPSCs evoked by extracellular stimulation at 0.1 Hz frequency before and after high-frequency stimulation (100 stimuli at 10 Hz frequency) in SV2B-deficient and SV2A/SV2B double-deficient neurons. *B, C*, Plot of either the absolute IPSC amplitudes (*B*) or the normalized amplitude (*C*) as a function of time (10 s) before and after high-frequency stimuli in SV2B KO (BKO) and SV2 double-KO (DKO) synapses. Data shown are means \pm SEMs (absolute responses but not the normalized responses are significantly different at the $p < 0.001$ level as tested by 2-way ANOVA).

Mutation of charged residues in TMR1 impairs SV2 targeting

Sequence analysis of the TMRs of SV2 isoforms and SVOP identified two negatively charged residues in TMR1 of these proteins (Janz et al., 1998; Janz and Südhof, 1999). The presence of charged residues in the middle of TMR1 and of multiple conserved glycine and proline residues in other TMRs fits the notion that SV2s could be transporters (Janz et al., 1999). Therefore, we mutated the two most conserved charged residues in a TMR1, namely aspartate 179 and glutamate 182, to alanine (D179A/E182A; referred to as the DA mutation). Immunoblotting of cultured neurons infected with lentivirus encoding SV2A with the

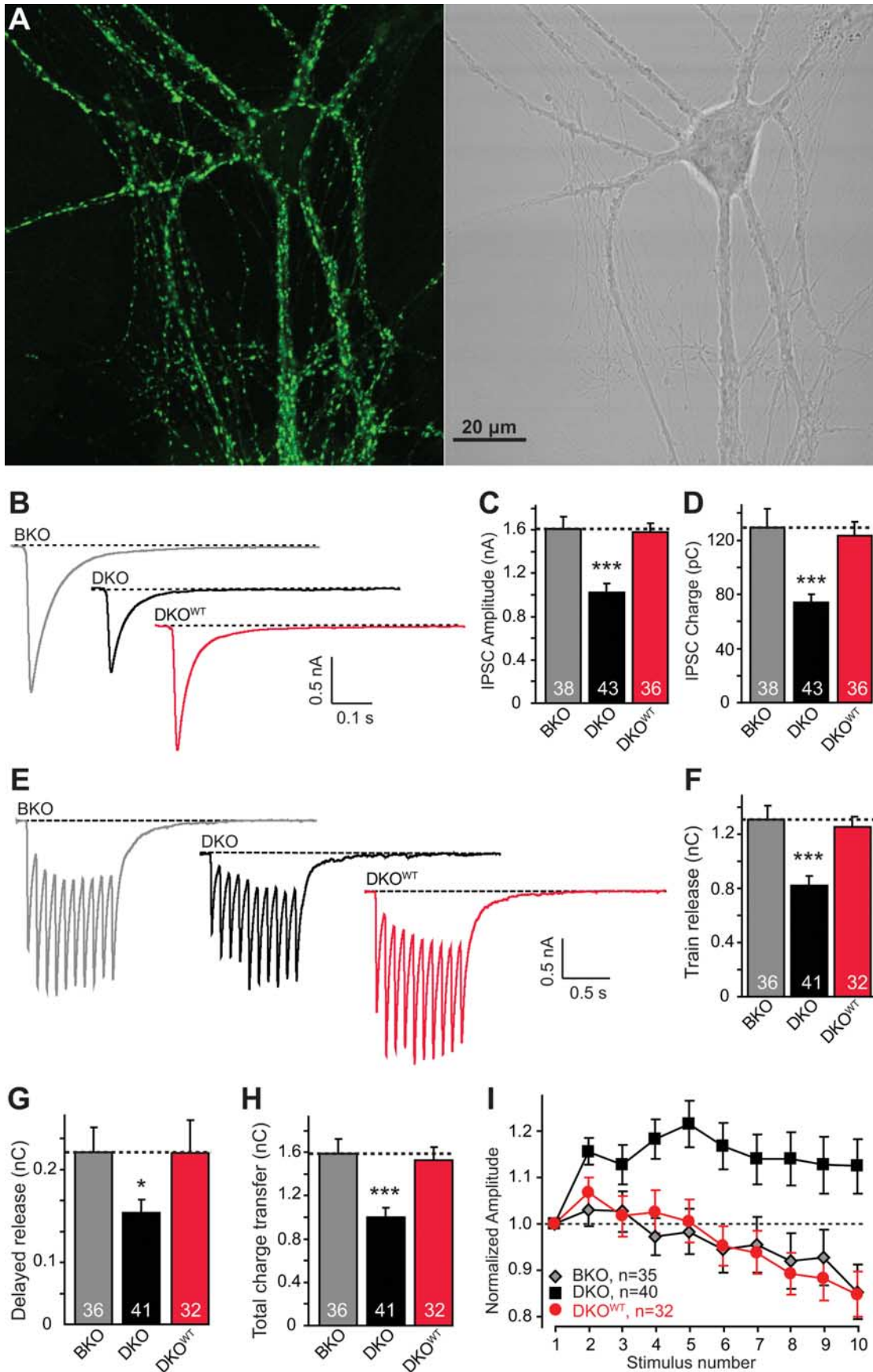


Figure 7. Rescue of the phenotype in SV2-deficient neurons by lentiviral expression of EGFP-tagged SV2A. *A*, Fluorescence (left) and phase-contrast (right) images of neurons infected with lentivirus expressing EGFP-SV2A. *B–D*, Representative traces (*B*), mean amplitudes (*C*), and charge transfers (*D*) of IPSCs evoked by extracellular stimulation at 0.1 Hz. Responses were monitored in cultured cortical neurons from littermate SV2B KO (BKO) and SV2A/SV2B double-KO mice, the latter either as naive neurons (DKO) or after infection with wild-type (*Figure legend continues*.)

mutant TMR1 revealed lower levels of expression (Fig. 8B,C), as long as with fluorescence image demonstrated that the mutant SV2A protein failed to go into synapses, but instead exhibited a diffuse pattern that filled the entire neuron (Fig. 10A). These observations indicate that the charged residues in TMR1 of SV2A may be required for the normal folding and targeting of SV2A. Not surprisingly, electrophysiological analyses revealed that the mutant TMR1 SV2A was unable to rescue responses evoked by single or repeated action potentials, and did not correct the short-term plasticity phenotype (Fig. 10B–G). Thus, the two charged residues in TMR1 are essential for the normal structure and function of SV2A.

Blocking SV2 glycosylation abolishes SV2 function

It was proposed that the three *N*-glycosylation consensus sequences in the large intravesicular loop of SV2 serve as glycosaminoglycan attachment sequences in SV2 (Janz et al., 1999), but the importance of this *N*-glycosylation, even its very dependence on the putative *N*-glycosylation sequences, was never examined. To test this question, and to probe the functional significance of SV2 glycosylation, we mutated the three asparagines in these consensus sequences to glutamines (Fig. 8A) (N498Q/N548Q/N573Q; referred to as the NQ mutation). Immunoblotting of the expressed intravesicular loop mutant of SV2A (SV2A^{NQ}) showed that the levels of the mutant protein were dramatically decreased, suggesting that without *N*-glycosylation, SV2 may not be targeted correctly and be unstable. Consistent with this notion, the localization of the mutant SV2A in neurons was strikingly abnormal: this mutant SV2A variant was not synaptic like wild-type SV2A, nor was it uniformly distributed throughout the cytoplasm like the TMR1 mutant, but present in larger concentrations, possibly aggregates, throughout the neuron (Fig. 11A). As expected from

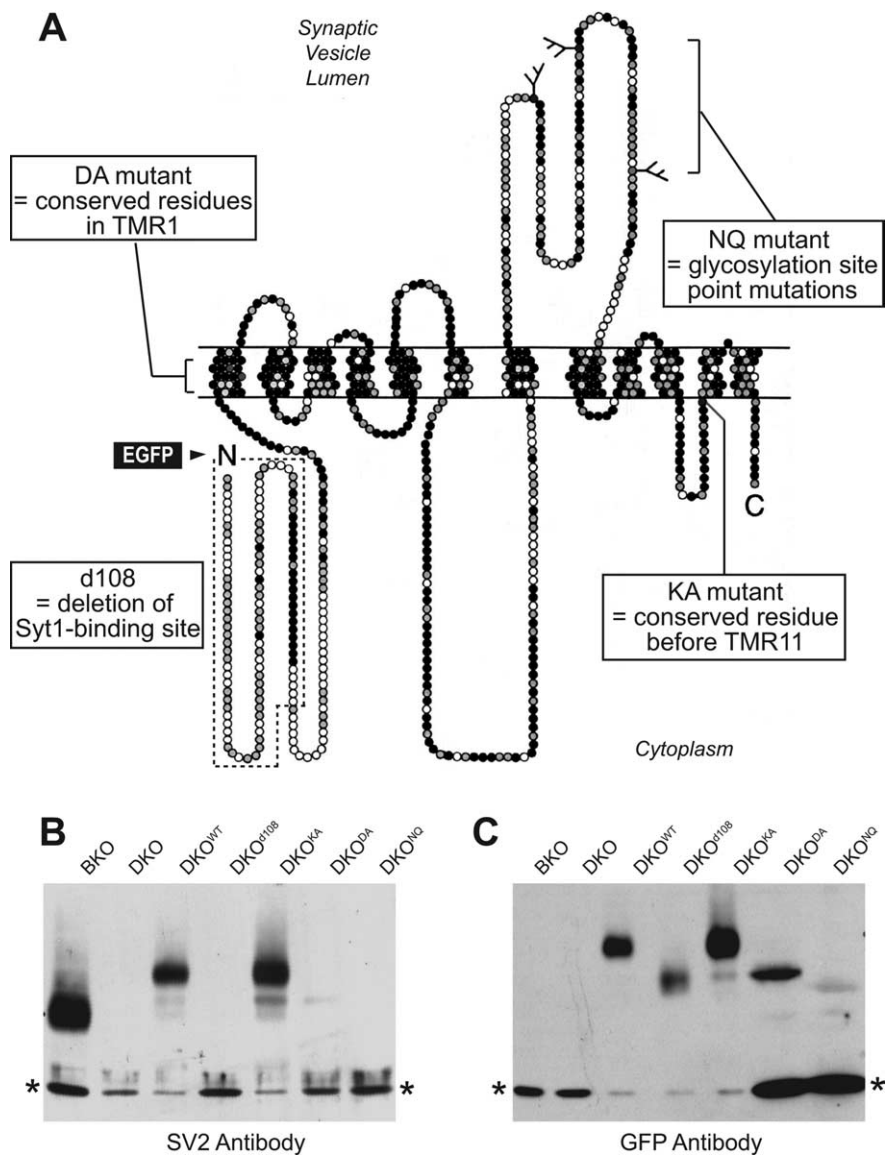


Figure 8. Structure and mutants of SV2A. **A**, Schematic diagram of the structure of SV2 proteins and location of mutants analyzed in Figures 7–10. Amino acid residues in the primary sequence of SV2A are indicated by circles, with 12 potential transmembrane regions (TMRs) predicted by sequence analyses. Residues that are conserved in SV2A, SV2B, and SV2C are shown in black, residues that are identical in at least two of the three isoforms in gray, and nonconserved residues in white. Branched lines show positions of N-linked carbohydrates. N and C termini are identified by letters (Janz et al., 1999). The positions of mutations are indicated: DA mutant (D179A/E182A), NQ mutant (N498Q/N548Q/N573Q), KA mutant (K694A), d108 mutant (deletion of residues 1–107). Fluorescent protein EGFP was fused to the N terminus of full-length or SV2A deletion protein as indicated by green arrow. **B**, **C**, Immunoblot analysis of the expression of wild-type EGFP-SV2A and of various EGFP-SV2A mutants in lentiviral-infected cultured neurons using antibodies to SV2 (**B**) and to GFP (**C**). All blots were additionally blotted for GDI as a loading control (bottom bands shown in the blot, indicated by asterisks); note that depending on expression levels, different amounts of protein were loaded on each lane, as is evident from the loading control.

←

(Figure legend continued.) EGFP-SV2A-expressing lentivirus (DKO^{WT}). Action potentials were evoked with a focal electrode in a bath solution containing 1 mM Ca²⁺ and 2 mM Mg²⁺. **E–H**, Representative traces (**E**) and summary graphs of the charge transfer during the stimulus train (train release, **F**), after the train (delayed release, **G**), and over the entire experiment (total charge transfer, **H**) in the same neurons described for panel **B** above. **I**, Plot of the normalized amplitude as a function of the stimulus number during the 10 Hz stimulus train in BKO and DKO neurons without or with rescue. All data shown are means ± SEMs (*n* = numbers shown in bar diagrams from at least 3 independent cultures; **p* < 0.05 and ****p* < 0.001 by Student's *t* test; in **I**, *n* = 35 for BKO neurons; *n* = 40 for DKO neurons; and *n* = 32 for DKO^{WT} neurons; values are significantly different between BKO and DKO neurons at the *p* < 0.0001 level as tested by 2-way ANOVA).

this mislocalization, we observed no rescue of SV2 function in neurons lacking SV2A and SV2B that expressed this mutant of SV2A (Fig. 11B–G). Thus, *N*-glycosylation of SV2A is essential for its normal processing and possibly folding.

Discussion

SV2 is an interesting but enigmatic synaptic vesicle protein. It is interesting because (1) it is highly homologous to bacterial sugar transporters, (2) its intravesicular sequence carries large glycosaminoglycan moieties, (3) its deletion in KO mice induces lethal epilepsy, and (4) it is the target of a widely used antiepileptic drug, levetiracetam (Buckley and Kelly, 1985; Bajjalieh et al., 1992,

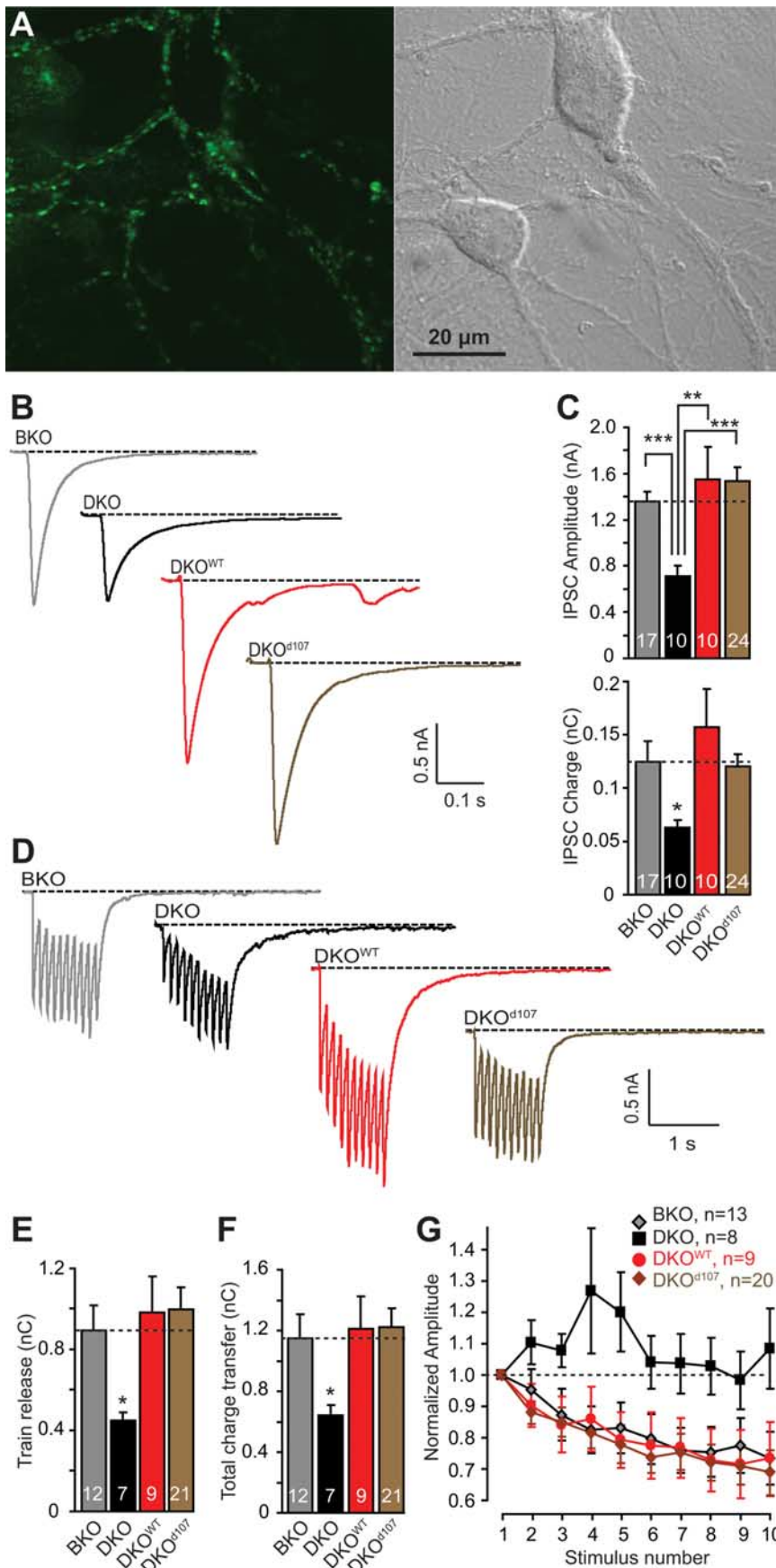


Figure 9. Rescue of the SV2 KO phenotype by mutant SV2A lacking the N-terminal 107 residues implicated in synaptotagmin binding. **A**, Fluorescence (left) and phase-contrast (right) images of neurons infected with lentivirus expressing d107 mutant EGFP-SV2A. **B**, **C**, Representative traces (**B**) and summary graphs (**C**) of IPSCs evoked by isolated action potentials in SV2B KO

1993; Feany et al., 1992; Gingrich et al., 1992; Crowder et al., 1999; Janz and Südhof, 1999; Janz et al., 1999; Lynch et al., 2004; Custer et al., 2006). It is enigmatic because (1) despite many hypotheses, SV2 has no validated function, as a transporter or otherwise, (2) it is even unclear whether its glycosaminoglycan modification is biologically important, (3) the initial characterization of its KO phenotype led to conflicting notions of where in synaptic vesicle exocytosis SV2 acts, and (4) its involvement in clinical epilepsy remains unclarified. In the present study, we attempted to address some of these issues, and aimed toward a better understanding of SV2 by studying its KO phenotype and the rescue of this phenotype by wild-type and mutant SV2. Our data reveal that SV2 acts at a previously unidentified step in synaptic vesicle exocytosis that links synaptic vesicle priming to Ca^{2+} triggering of fusion, suggesting that SV2 boost the Ca^{2+} responsiveness of primed vesicles. Moreover, we demonstrate that both the transmembrane structure and the glycosaminoglycan modification are essential for SV2 function, whereas other suggested features, especially its synaptotagmin-binding site, are not.

Dissection of the SV2 KO phenotype

Consistent with earlier studies of SV2-deficient excitatory synapses (Crowder et al., 1999; Janz et al., 1999; Custer et al., 2006), we observed that deletion of SV2 impairs evoked neurotransmitter release in inhibitory synapses (Figs. 1–4), and enhances synaptic facilitation during 10 Hz stimulus trains (Figs. 4, 5). Specifically, we made six observations.

First, SV2 acts similarly in inhibitory synapses (this work) and excitatory synapses (previous studies).

Second, deletion of SV2 equally de-

neurons (BKO) or SV2A/B double-KO neurons without rescue (DKO) or after rescue with wild-type SV2A (DKO^{WT}) or d107 mutant SV2A (DKO^{d107}). **D–F**, Representative traces (**D**) and summary graphs of train release (**E**) and total release (**F**) of BKO neurons and naive and rescued DKO neurons stimulated at 10 Hz for 1 s. **G**, Plot of the relative amplitude of synaptic responses during a 10 Hz stimulus train as a function of stimulus number in BKO neurons and naive and rescued DKO neurons. All data shown are means ± SEMs (*n* = numbers shown in bar diagrams from at least 3 independent cultures; **p* < 0.05, ***p* < 0.01, and ****p* < 0.001 by Student's *t* test; in **G**, *n* = 13 for BKO synapses; *n* = 8 for DKO synapses; *n* = 9 for rescued DKO^{WT} synapses; and *n* = 20 for DKO^{d107} neurons; values are significantly different between BKO and DKO neurons, but not between BKO and rescued DKO neurons, at the *p* < 0.0001 level as tested by 2-way ANOVA).

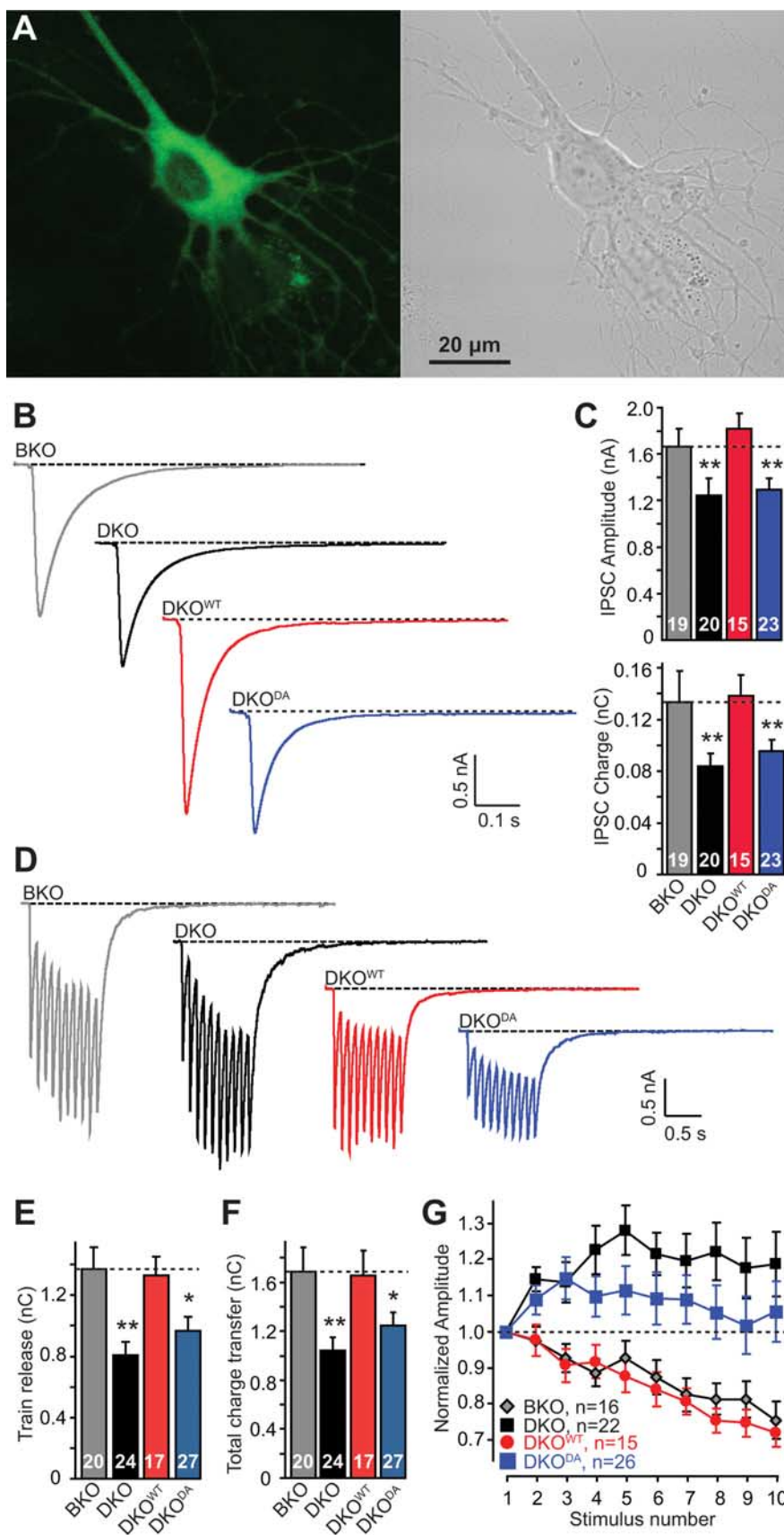


Figure 10. Lack of rescue of the SV2 KO phenotype by DA mutant SV2A containing a double amino acid substitution in TMR1 (D179A/E182A). **A**, Fluorescence (left) and phase-contrast (right) images of neurons infected with lentivirus expressing DA mutant EGFP-SV2A. **B**, **C**, Representative traces (**B**) and summary graphs (**C**) of IPSCs evoked by isolated action potentials in SV2B KO neurons (BKO) or SV2A/B double-KO neurons without rescue (DKO) or after rescue with wild-type SV2A (DKO^{WT}) or DA mutant

increased synchronous and asynchronous release evoked by isolated or repeated action potentials (Figs. 2, 4).

Third, deletion of SV2 did not decrease the size of the RRP as confirmed in four different experiments: (1, 2) measurements of the RRP induced by hypertonic sucrose in excitatory and in inhibitory synapses; (3) measurements of the RRP induced by hypertonic sucrose in inhibitory synapses after 24 h of silencing with TTX; and (4) measurements of the RRP induced by Ca²⁺ influx mediated by ionomycin in inhibitory synapses (Figs. 2, 3).

Fourth, consistent with a normal RRP size, the SV2 deletion did not alter mini frequencies or amplitudes in excitatory or inhibitory synapses (Fig. 1).

Fifth, the SV2 deletion also did not change the apparent Ca²⁺ affinity of synapses. Again, four lines of evidence support this conclusion: there was no change in the Ca²⁺ dependence of release (Fig. 2), the ratio of synchronous to asynchronous release was unaltered, the kinetics of ionomycin-induced release was not different in SV2-deficient synapses (Fig. 3), and EGTA-AM had the same relative effect on wild-type and SV2-deficient synapses (Fig. 5).

Sixth, SV2-deficient synapses exhibited enhanced facilitation during repetitive stimulation (Fig. 4). This phenotype was rescued by EGTA-AM, a drug that lowers the bulk cytoplasmic Ca²⁺ concentration, whereas EGTA-AM did not alter the relative decrease in release in the SV2-deficient synapses (Fig. 5). Thus, the increased facilitation but not the loss of release in SV2-deficient synapses likely results from relatively higher accumulation of residual Ca²⁺ during a stimulus train.

Our results generally agree with previous analyses of SV2-deficient synapses in autapses (Janz et al., 1999; Custer et al., 2006). Different from Custer et al. (2006), however, we did not observe a decrease in

SV2A (DKO^{DA}). **D–F**, Representative traces (**D**) and summary graphs of train release (**E**) and total release (**F**) of BKO neurons and naive and rescued DKO neurons stimulated at 10 Hz for 1 s. **G**, Plot of the relative amplitude of synaptic responses during a 10 Hz stimulus train as a function of stimulus number in BKO neurons and naive and rescued DKO neurons. All data shown are means ± SEMs (n = numbers shown in bar diagrams from at least 3 independent cultures; * p < 0.05 and ** p < 0.01 by Student's t test; in **G**, n = 16 for BKO neurons; n = 22 for DKO neurons; n = 15 for DKO^{WT} neurons; and n = 26 for DKO^{DA} neurons; values are significantly different between BKO and DKO neurons, but not between DKO and DKO^{DA} rescued neurons, at the p < 0.0001 level as tested by 2-way ANOVA).

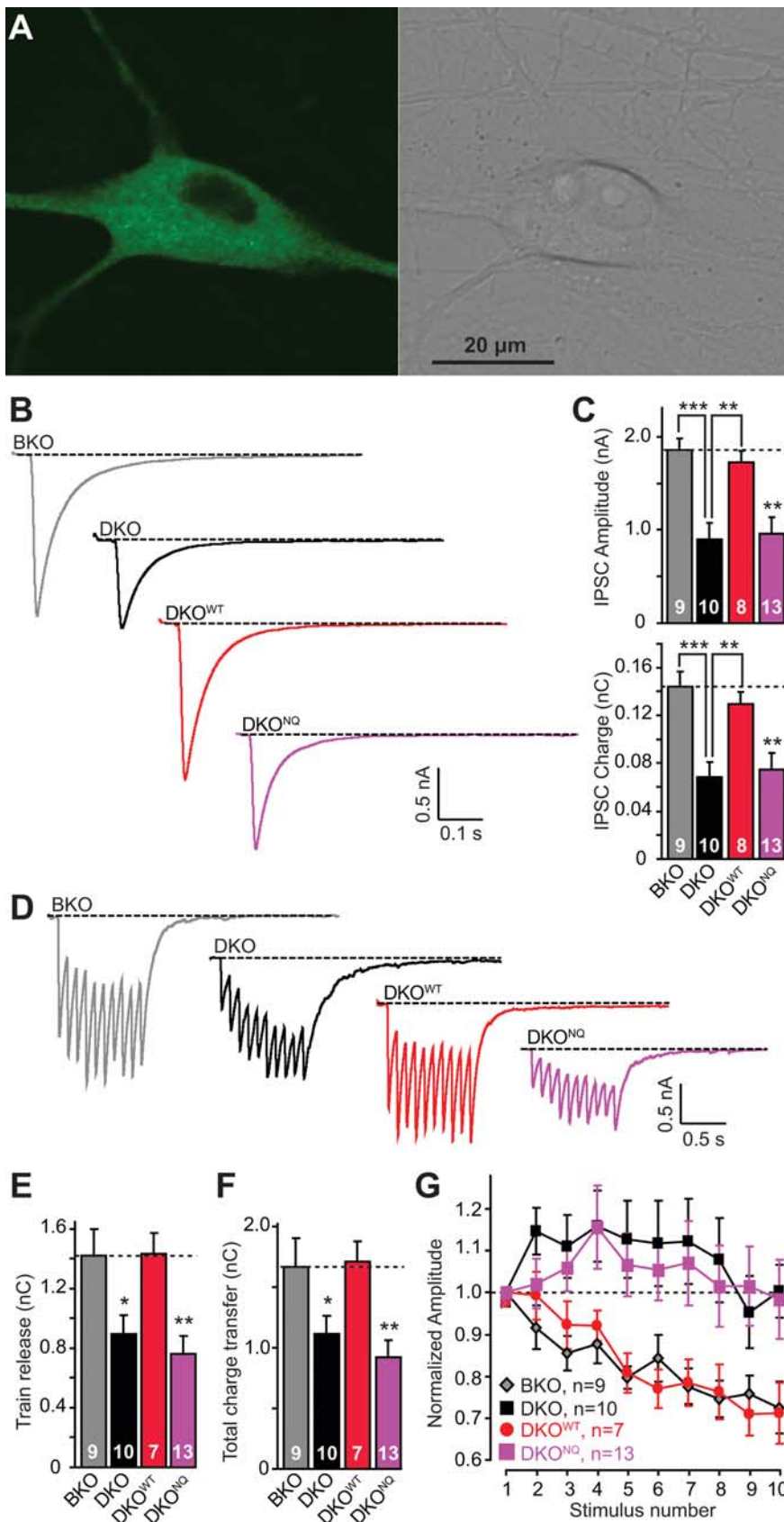


Figure 11. Lack of rescue of the SV2 KO phenotype by NQ mutant SV2A in which the *N*-glycosylation sites in the intravesicular loop were substituted. **A**, Fluorescence (left) and phase-contrast (right) images of neurons infected with lentivirus expressing NQ mutant EGFP-SV2A (NQ mutant carries three substitutions: N498Q/N548Q/N573Q). **B**, **C**, Representative traces (**B**) and summary graphs (**C**) of IPSCs evoked by isolated action potentials in SV2B KO neurons (BKO) or SV2A/B double-KO neurons without rescue (DKO) or after rescue with wild-type SV2A (DKO^{WT}) or NQ mutant SV2A (DKO^{NQ}). **D–F**, Representative traces (**D**) and

the RRP, or a rescue of the release phenotype by accumulating Ca²⁺ during stimulus trains. The lack of a change in the RRP by deletion of SV2 is supported by the finding that the mini frequency is unchanged (Fig. 1), as also previously reported by Custer et al. (2006). A possible explanation for the lack of a change in RRP could have been that the continuous network activity in our cultures creates a permanent state of “accumulating Ca²⁺” that might rescue the phenotype. However, chronic treatment of our cultures with TTX, which blocks continuous network activity, did not alter the lack of an RRP phenotype (Fig. 2). Another possible explanation for the differences between our results and those of Custer et al. (2006) is that inhibitory versus excitatory synapses were analyzed. However, the decrease in release we observed in inhibitory synapses precisely matches that detected by Custer et al. (2006) in excitatory synapses, suggesting that the SV2 KO phenotype is the same between the two types of synapses. Moreover, we also measured the RRP in excitatory synapses and found no change. A third possible explanation for the discrepancy in phenotype we observed versus that reported by Custer et al. (2006) is that we study synapses formed between neurons, whereas Custer et al. (2006) examined autapses. This hypothesis is consistent with the fact that the dynamics of accumulating Ca²⁺ during a stimulus train is likely to differ between autapses and synapses formed between neurons because in the former, presynaptic and postsynaptic neurons are one and the same, whereas in the latter, only the presynaptic neuron is excited. Last, the difference in results may be due to the fact that we studied cortical neurons whereas Custer et al. (2006) analyzed hippocampal neurons. Although SV2A is ubiquitously expressed in all neurons, recording from different types of neurons may be another reason for the different observations.

←

summary graphs of train release (**E**) and total release (**F**) of BKO neurons and naive and rescued DKO neurons stimulated at 10 Hz for 1 s. **G**, Plot of the relative amplitude of synaptic responses during a 10 Hz stimulus train as a function of stimulus number in BKO neurons and naive and rescued DKO neurons. All data shown are means ± SEMs (*n* = numbers shown in bar diagrams from at least 3 independent cultures; **p* < 0.05, ***p* < 0.01, and ****p* < 0.001 by Student's *t* test; in **G**, *n* = 9 for BKO synapses; *n* = 10 for DKO synapses; *n* = 7 for DKO^{WT} synapses; and *n* = 13 for DKO^{NQ} synapses; values are significantly different between BKO and DKO neurons, but not between DKO and DKO^{NQ} rescued DKO neurons, at the *p* < 0.0001 level as tested by 2-way ANOVA).

Structure–function analysis of SV2A

The three SV2 isoforms containing four highly conserved features: the N-terminal sequence bearing the epitope of the original SV2 monoclonal antibody that reacts with all isoforms; the membrane-associated sequences with the 12 TMRs and the small loops connecting them; the large intravesicular loop that is N-glycosylated but otherwise exhibits major variations between isoforms; and the large cytoplasmic loop (Janz et al., 1999). Three of these four conserved elements were previously associated with functional hypotheses that were tested in the present experiments: the N-terminal sequence was shown to bind synaptotagmin (Schivell et al., 1996, 2005; Pyle et al., 2000) (but see Lazzell et al., 2004), the transmembrane sequences were hypothesized to function as transporters due to their homology to sugar transporter proteins (Bajjalieh et al., 1992; Feany et al., 1992; Gingrich et al., 1992; Bajjalieh et al., 1993; Janz and Südhof, 1999), and the glycosylated intravesicular sequence was thought to mediate vesicle stability and neurotransmitter storage (Scranton et al., 1993; Janz and Südhof, 1999; Reigada et al., 2003). Our data reveal that the N-terminal synaptotagmin-binding sequence containing the SV2-antibody epitope is dispensable for the ability of the SV2A to rescue the SV2 KO phenotype (Fig. 9), but that mutations of conserved charged residues in TMR1 or of the N-glycosylation sites in the intravesicular sequence loop of SV2A abolished its normal processing (Figs. 10, 11). Both of these mutations destabilized SV2A as indicated by decreased expression levels in infected culture neurons, and abolished the targeting of SV2 to synapses as indicated by imaging in neurons expressing the mutant SV2A. Thus, it is likely that these mutations inactivated SV2A by impairing the folding and targeting of SV2A, suggesting that one of the functions of the sequences involved is to allow the correct conformation of SV2A required for its normal transport into synaptic vesicles.

The function of SV2

Our data clarify old hypotheses regarding SV2 function, but also raise new questions. Specifically, the lack of rescue of the neurotransmitter release phenotype by the intracellular Ca^{2+} buffer EGTA-AM (Fig. 4), manifested in the identical relative suppression of synaptic transmission by EGTA-AM in control and SV2-deficient synapses, suggests that SV2 does not primarily function as a Ca^{2+} transporter during stimulus trains as we hypothesized earlier (Janz et al., 1999), but acts even at resting Ca^{2+} concentrations. The fact that the phenotype can be rescued by expression of EGFP-tagged SV2A demonstrates that it is caused by a functional and not a developmental change (Fig. 7). The lack of an effect of the SV2 deletion on the apparent Ca^{2+} affinity of release and the full rescue of release upon expression of N-terminally deleted SV2 indicate that synaptotagmin binding by SV2 is not functionally essential. Similarly, the lack of an effect of the SV2 deletion on the RRP size indicates that SV2 is not a priming factor.

So what does SV2 do? The release phenotype we observed in SV2-deficient synapses does not conform to current models of release. We show that the SV2 deletion causes a substantial loss of release that operates downstream of synaptic vesicle priming, but upstream of Ca^{2+} triggering of release. Both conclusions were supported by multiple lines of evidence as described above. The most parsimonious and plausible hypothesis to account for this discrepant phenotype is that SV2 enhances the Ca^{2+} responsiveness of primed synaptic vesicles. As such an “efficiency factor,” SV2 may not be required in invertebrate synapses, accounting for

its relatively recent evolutionary appearance. This hypothesis accounts for both the decreased release and the enhanced facilitation phenotype (which would be due to increased availability of vesicles for triggering by accumulating residual Ca^{2+}). An alternative hypothesis would be that SV2 is essential for normal filling of synaptic vesicles with transmitters, which would be consistent with its transporter-like structure but is contradicted by the normal mini amplitudes in SV2-deficient synapses. Another alternative hypothesis is that SV2 is essential for normal functions of plasmalemmal voltage-gated channels, i.e., for action potential generation or Ca^{2+} channel opening, but the strict localization of SV2 to synaptic vesicles argues against such a role. Thus, although much remains to be done, it appears likely that SV2 functions in exocytosis as a trafficking protein that enhances the Ca^{2+} responsiveness of vesicles.

References

- Bajjalieh SM, Peterson K, Shinghal R, Scheller RH (1992) SV2, a brain synaptic vesicle protein homologous to bacterial transporters. *Science* 257:1271–1273.
- Bajjalieh SM, Peterson K, Linial M, Scheller RH (1993) Brain contains two forms of synaptic vesicle protein 2. *Proc Natl Acad Sci U S A* 90:2150–2154.
- Bajjalieh SM, Frantz GD, Weimann JM, McConnell SK, Scheller RH (1994) Differential expression of synaptic vesicle protein 2 (SV2) isoforms. *J Neurosci* 14:5223–5235.
- Buckley K, Kelly RB (1985) Identification of a transmembrane glycoprotein specific for secretory vesicles of neural and endocrine cells. *J Cell Biol* 100:1284–1294.
- Crowder KM, Gunther JM, Jones TA, Hale BD, Zhang HZ, Peterson MR, Scheller RH, Chavkin C, Bajjalieh SM (1999) Abnormal neurotransmission in mice lacking synaptic vesicle protein 2A (SV2A). *Proc Natl Acad Sci U S A* 96:15268–15273.
- Custer KL, Austin NS, Sullivan JM, Bajjalieh SM (2006) Synaptic vesicle protein 2 enhances release probability at quiescent synapses. *J Neurosci* 26:1303–1313.
- Dong M, Yeh F, Tepp WH, Dean C, Johnson EA, Janz R, Chapman ER (2006) SV2 is the protein receptor for botulinum neurotoxin A. *Science* 312:592–596.
- Feany MB, Lee S, Edwards RH, Buckley KM (1992) The synaptic vesicle protein SV2 is a novel type of transmembrane transporter. *Cell* 70:861–867.
- Fernández-Chacón R, Königstorfer A, Gerber SH, García J, Matos MF, Stevens CF, Brose N, Rizo J, Rosenmund C, Südhof TC (2001) Synaptotagmin I functions as a calcium regulator of release probability. *Nature* 410:41–49.
- Gingrich JA, Andersen PH, Tiberi M, el Mestikawy S, Jorgensen PN, Fremeau RT Jr, Caron MG (1992) Identification, characterization, and molecular cloning of a novel transporter-like protein localized to the central nervous system. *FEBS Lett* 312:115–122.
- Janz R, Südhof TC (1999) SV2C is a synaptic vesicle protein with an unusually restricted localization: anatomy of a synaptic vesicle protein family. *Neuroscience* 94:1279–1290.
- Janz R, Hofmann K, Südhof TC (1998) SVOP, an evolutionarily conserved synaptic vesicle protein, suggests novel transport functions of synaptic vesicles. *J Neurosci* 18:9269–9281.
- Janz R, Goda Y, Geppert M, Missler M, Südhof TC (1999) SV2A and SV2B function as redundant Ca^{2+} regulators in neurotransmitter release. *Neuron* 24:1003–1016.
- Katz B (1969) The release of neural transmitter substances. Liverpool, UK: Liverpool UP.
- Laemmli UK (1970) Cleavage of structural proteins during the assembly of the head of bacteriophage T4. *Nature* 227:680–685.
- Lazzell DR, Belizaire R, Thakur P, Sherry DM, Janz R (2004) SV2B regulates synaptotagmin 1 by direct interaction. *J Biol Chem* 279:52124–52131.
- Lynch BA, Lambeng N, Nocka K, Kensel-Hammes P, Bajjalieh SM, Matagne A, Fuks B (2004) The synaptic vesicle protein SV2A is the binding site for the antiepileptic drug levetiracetam. *Proc Natl Acad Sci U S A* 101:9861–9866.

- Mahrhold S, Rummel A, Bigalke H, Davletov B, Binz T (2006) The synaptic vesicle protein 2C mediates the uptake of botulinum neurotoxin A into phrenic nerves. *FEBS Lett* 580:2011–2014.
- Maximov A, Südhof TC (2005) Autonomous function of synaptotagmin 1 in triggering synchronous release independent of asynchronous release. *Neuron* 48:547–554.
- Maximov A, Pang ZP, Tervo DG, Südhof TC (2007) Monitoring synaptic transmission in primary neuronal cultures using local extracellular stimulation. *J Neurosci Methods* 161:75–87.
- Pyle RA, Schivell AE, Hidaka H, Bajjalieh SM (2000) Phosphorylation of synaptic vesicle protein 2 modulates binding to synaptotagmin. *J Biol Chem* 275:17195–17200.
- Reigada D, Díez-Pérez I, Gorostiza P, Verdaguer A, Gómez de Aranda I, Pineda O, Vilarrosa J, Marsal J, Blasi J, Aleu J, Solsona C (2003) Control of neurotransmitter release by an internal gel matrix in synaptic vesicles. *Proc Natl Acad Sci U S A* 100:3485–3490.
- Rosenmund C, Stevens CF (1997) The rate of aldehyde fixation of the exocytotic machinery in cultured hippocampal synapses. *J Neurosci Methods* 76:1–5.
- Schivell AE, Batchelor RH, Bajjalieh SM (1996) Isoform-specific, calcium-regulated interaction of the synaptic vesicle proteins SV2 and synaptotagmin. *J Biol Chem* 271:27770–27775.
- Schivell AE, Mochida S, Kensel-Hammes P, Custer KL, Bajjalieh SM (2005) SV2A and SV2C contain a unique synaptotagmin-binding site. *Mol Cell Neurosci* 29:56–64.
- Scranton TW, Iwata M, Carlson SS (1993) The SV2 protein of synaptic vesicles is a keratan sulfate proteoglycan. *J Neurochem* 61:29–44.
- Südhof TC (2004) The synaptic vesicle cycle. *Annu Rev Neurosci* 27:509–547.
- Sun J, Pang ZP, Qin D, Fahim AT, Adachi R, Südhof TC (2007) A dual-Ca²⁺-sensor model for neurotransmitter release in a central synapse. *Nature* 450:676–682.
- Xu T, Bajjalieh SM (2001) SV2 modulates the size of the readily releasable pool of secretory vesicles. *Nat Cell Biol* 3:691–698.